Chinese Chemical Letters 32 (2021) 2773–2776

Contents lists available at ScienceDirect

Chinese Chemical Letters

journal homepage: www.elsevier.com/locate/cclet

Communication

Pyrrole/macrocycle/MOF supramolecular co-assembly for flexible solid state supercapacitors

Shan-Shan Jia, Wen-Shi Xu, Yong Chen*, Yu Liu*

College of Chemistry, State Key Laboratory of Elemento-Organic Chemistry, Nankai University, Tianjin 300071, China

ARTICLE INFO

Article history:
Received 6 January 2021
Received in revised form 24 February 2021
Accepted 1 March 2021
Available online 3 March 2021

Keywords:
Supramolecular assemblies
Macrocycle
Conductive polymers
Electrochemical performance
Cationic radical

ABSTRACT

Supramolecular assemblies constructed through the encapsulation of conductive polymers (CPs) by macrocyclic molecules have attracted increasing interest in the fields of supramolecular chemistry and electrochemistry. In this work, an effective strategy was reported to improve the stability and conductivity of CPs by electrochemically constructing different supramolecular assemblies composed of macrocycles and CPs. Typically, we uploaded zinc-based MOF (ZIF-8) onto carbon nanotube film (CNTF) and further electrically deposited macrocycles and CPs to gain the flexible conductive electrodes. Herein, five different supramolecular macrocycles, including α-cyclodextrin (α-CD), sulfato-β-cyclodextrin (SCD), sulfonatocalix[4]arene (SC[4]), cucurbit[6]uril (CB[6]) and cucurbit[7]uril (CB[7]) were utilized and the electrochemical performances of the assembly electrodes increased in an order of α-CD < SCD < SC[4] < CB[6] < CB[7], significantly improving the areal capacitance up to 1533 mF/cm^2. This strategy may provide a new way for the application of macrocyclic supramolecules in electrochemical systems.

Recently, the research on the supramolecular assemblies of macrocyclic molecules and polymers [1–3], especially the conductive polymers (CPs) [4], has attracted more and more attention in the fields of supramolecular chemistry and electrochemistry owing to the specific properties of assemblies, which are totally different from the traditional conductive polymers. Supramolecular assemblies [5,6] are intelligent response materials [7] constructed by non-covalent bonds, such as hydrogen bonds, π–π stacking, hydrophobic interaction, van der Waals forces, metal-ligand interaction, and electrostatic interaction, having attracted more and more attention [8,9]. Due to the excellent physical and chemical properties such as self-assembly [10], responsiveness [11], synergy and regeneration [12], supramolecular assemblies exhibit distinctive application prospects in supramolecular functional materials and devices, molecular devices and machines at the nanometer and molecular scales [13,14], targeted drug release [15,16], electrochemistry and highly selective catalysts [17]. The early exploration on such supramolecular assemblies is usually based on cyclodextrins [18] or crown ethers [19]. Recently, cucurbit[n]uril (CB[n], n is usually 6–8) as the main molecule to fabricate the assemblies has also been reported [20,21], which possesses remarkable binding abilities towards many cationic guests. In consequence of the cucurbituril cavity surrounded by carbonyl groups [22] and the cationic bonding sites, positively charged molecules can be encapsulated through dipole interaction [23] and hydrogen bonding [24]. Compared with cyclodextrin or other macrocyclic compounds, cucurbituril has a more rigid structure [25]. When combined with a guest, cucurbituril will not change its shape in order to adapt to the guest, thus reflecting higher selection specificity [26] and extremely high complex constant, which makes cucurbituril play an irreplaceable role in supramolecular chemistry. Kim *et al.* [27] as well as Tuncel *et al.* [28,29] first attempted to construct an assembly with polymer chains and cucurbituril. The research on assemblies of cucurbituril and conductive polymers [30] has received increasing interest. Liu *et al.* [4] reported a pseudorotaxane constructed by polyaniline (PANI) and CB[7], which had favorable water solubility and the radical cation [31] had superior stability as a consequence of the complexation with CB[7], compared with free PANI. This complexation led to a lower attenuation rate, a relatively low attenuation ratio of the radical cation, and lower first oxidation and reduction potentials contrasted to those of free PANI. These advantages will allow the further research of PANI-based supramolecular assemblies in numerous fields, which also inspire the investigation on the assemblies of macrocycles and conductive polymers.

In this work, we introduced several types of macrocycles into the construction process of CPs to fabricate marcocycle-improved CPs, taking full use of the advantages of macrocyclic compounds.

* Corresponding authors.
E-mail addresses: chenyong@nankai.edu.cn (Y. Chen), yuliu@nankai.edu.cn (Y. Liu).

https://doi.org/10.1016/j.cclet.2021.03.002

Then, we had utilized cyclic voltammetry (CV), electrochemical impedance spectroscopy (EIS), galvanostatic charge-discharge (GCD) and scanning electron micrograph (SEM) to research the electrochemical performance and morphology of the electrode. In addition, ^{1}H NMR, 2D rotating frame overhauser enhancement spectroscopy (2D ROESY), isothermal titration calorimetry (ITC) were applied to investigate the structural information of the assemblies. After electrochemical deposition, the independent MOFs were interosculated and contacted by the assemblies that served as bridges for electrons conveyance among MOFs and significantly promoted the oxidation performance of the system. An exceptional effect can be noticed in this method.

A series of assemblies were fabricated which were composed of supramolecular macrocycles and an *in-situ* formed conductive polymer-polypyrrole (PPY), where several types of macrocyclic molecules, such as α-cyclodextrin (α-CD), sulfato-β-cyclodextrin (SCD), sulfonatocalix[4]arene (SC[4]), cucurbit[6]uril (CB[6]) and cucurbit[7]uril (CB[7]) have been utilized, along with ZIF-8 [32], a Zn-based MOF, as the electrical charge storage materials, and carbon nanotube film (CNTF) [33] was used as both substrate and flexible electronic devices. Firstly, ZIF-8 was deposited on CNTF, and then electrochemically interconnected in the presence of macrocycle/PPY supramolecular assemblies, and thus the gained electrode was named as X-PPY-ZIF-8-CNTF (X represented different supramolecular macrocycles). As a consequence of the distinctive stability of the radical cation in CB[7]-PPY assemblies and the exceptional water solubility of CB[7], compared with other assemblies, CB[7]-PPY electrode had advantageous electrochemical properties and excellent cycle stability (Table 1). Such a hybrid-structured electrode integrated high stability from CB[7] and marvelous pseudocapcitance generated by PPY. Compared with PPY-ZIF-8-CNTF, an extraordinary improvement of areal capacitance for CB[7]-PPY-ZIF-8-CNTF in a three-electrode system was realized (from 855 mF/cm^2 to 1533 mF/cm^2 at 5 mV/s). At the same time, the CB[7]-PPY-ZIF-8-CNTF electrode could retain more than 83% of its primary capacitance after 2000 cycles. These effects will benefit the extensive application of CP-based assemblies in both fields of supramolecular chemistry and electrochemistry.

The fabrication process of X-PPY-ZIF-8-CNTF electrode is illustrated in Scheme 1. Firstly, a slurry of 70 wt% ZIF-8 with 20 wt% acetylene black and 10 wt% poly(vinylidene fluoride) (PVDF) binder in *N*-methylpyrrolidone (NMP) was coated on CNTF. The obtained ZIF-8/carbon nanotube film electrode (named as ZIF-8-CNTF) still maintained the satisfactory mechanical flexibility and strength. In SEM images, ZIF-8 crystals presented as particles with sizes around 30−50 nm and evenly distributed upon the surface of the carbon nanotube film fibers (Fig. 1b and Fig. S1 in Supporting information). Secondly, X and pyrrole were electrochemically co-polymerized on the surface of ZIF-8-CNTF to obtain X-PPY-ZIF-8-CNTF. As shown in Fig. S2 (Supporting information), ZIF-8 crystals were interosculated by conductive X-PPY assemblies. Then, the gained X-PPY-ZIF-8-CNTF was dried at 80 °C. The electrochemical characterization of PPY-ZIF-8-CNTF and X-PPY-ZIF-8-CNTF electrodes was carried out in a three-electrode system, with 3 mol/L potassium chloride (KCl) as the electrolyte. The reference and the counter electrodes were saturated calomel electrode and Pt electrode respectively. The electrochemical properties of X-PPY-ZIF-8-CNTF and PPY-ZIF-8-CNTF electrodes were shown in Fig. 2. The CV curves demonstrated that among these assemblies, SCD-PPY-ZIF-8-CNTF and SC[4]-PPY-ZIF-8-CNTF electrodes had better CV curves and larger areal capacitance than PPY-ZIF-8-CNTF and α-CD-PPY-ZIF-8-CNTF electrodes, probably because that the sulfonate anions on SCD and SC[4] molecules can stabilize the cationic free radical of pyrrole, and thus increase the deposition efficiency. As a consequence of the carbonyl groups and cation bonding sites of cucurbituril molecule, CB[6] had a better binding ability with

Table 1
The areal capacitance of the flexible electrode of different supramolecular assemblies.

Assembly electrodes	Areal capacitance (mF/cm^2)
Original CP (PPY)	855
α-CD-PPY	868
SCD-PPY	958
SC[4]-PPY	1053
CB[6]-PPY	1180
CB[7]-PPY	1533

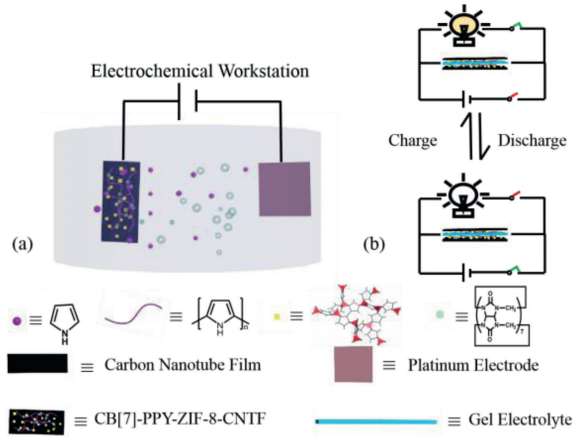

Scheme 1. (a) Preparation of CB[7]-PPY-ZIF-8-CNTF; (b) Charge and discharge process of supercapacitor.

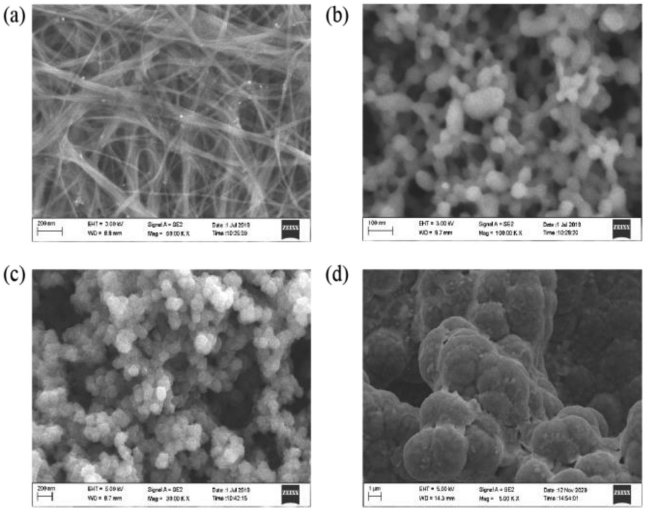

Fig. 1. Scanning electron micrograph of (a) CNTF, (b) ZIF-8-CNTF electrode, (c) PPY-ZIF-8-CNTF electrode, (d) CB[7]-PPY-ZIF-8-CNTF electrode.

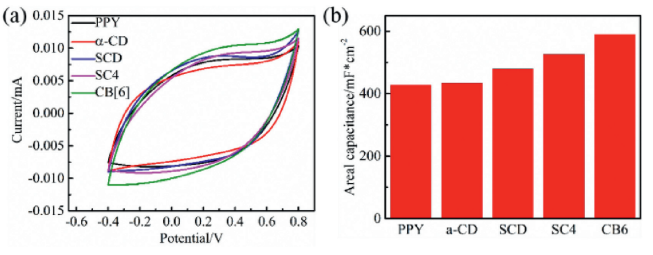

Fig. 2. Electrochemical characterization results of five kinds of electrodes: (a) Cyclic voltammetry curves at a scanning speed of 50 mV/s; (b) Areal capacitance at 5 mV/s.

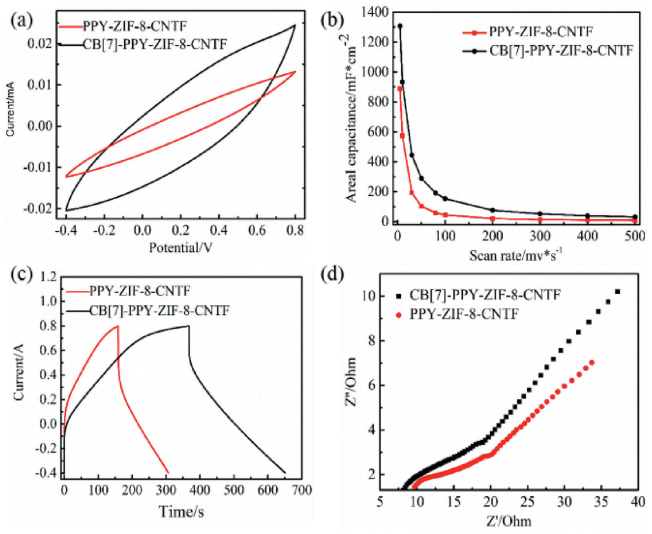

Fig. 3. The electrochemical properties of CB[7]-PPY-ZIF-8-CNTF and PPY-ZIF-8-CNTF electrodes: (a) The cyclic voltammetry curves at scanning speed of 50 mV/s; (b) The areal capacitance curves; (c) Constant current charge and discharge curves at a charge current of 6 mA/cm^2; (d) The impedance diagram.

pyrrole radical cation. Therefore, compared with other macrocyclic molecules, CB[6]-PPY-ZIF-8-CNTF had the largest CV curve area and the highest areal capacitance under the same conditions, as shown in Figs. 2a and b. It was worth noting that the α-CD had no positive effect on the areal capacitance of the PPY-ZIF-8-CNTF electrode, but the others did. This result indicated that the main reason for the promotion of the electrochemical performance of the X-PPY-ZIF-8-CNTF electrode should be attributed to the stabilization of SCD, SC[4] and CB[6] towards the cationic radical of pyrrole and the increase of the electrodeposition efficiency.

Considering that the poor solubility of CB[6] in water will reduce its stabilization effect on pyrrole radical to some extent, we chose CB[7] that was more soluble to further improve the electrical properties. As shown in Fig. 3, the CB[7]-PPY-ZIF-8-CNTF electrode represented the good areal capacitance up to 1533 mF/cm^2, that is two times higher than that of PPY-ZIF-8-CNTF (855 mF/cm^2) at scan speed of 5 mV/s, accompanied by the greater CV curve, longer discharge time and lower electrochemical impedance than PPY-ZIF-8-CNTF electrode. Fig. 3d illustrated the Nyquist plots of CB[7]-PPY-ZIF-8-CNTF and PPY-ZIF-8-CNTF respectively. In the low frequency region, CB[7]-PPY-ZIF-8-CNTF had a larger slope, which was nearly paralleled to the imaginary axis, illustrating the favorable capacitive behavior compared with PPY-ZIF-8-CNTF electrode. In the high frequency region, the intercept of CB[7]-PPY-ZIF-8-CNTF was smaller, demonstrating that CB[7]-PPY-ZIF-8-CNTF electrode had the lower interface contact resistance and charge transfer resistance.

This jointly confirmed the advantageous electrochemical properties of CB[7]-PPY-ZIF-8-CNTF. A possible reason may be the construction of assemblies consisted of PPY and CB[7] could enhance the cationic radical stability of PPY to further improve its conductivity, because the graph of areal capacitance with different scan rate (Fig. 3b) displayed that CB[7]-PPY-ZIF-8-CNTF had higher areal capacitance than PPY-ZIF-8-CNTF electrode. In addition, the improved water solubility of PPY by the solubilization of CB[7] may also contribute to the good electrochemical performance of assembly.

The above results indicated that the supramolecular assemblies system constructed by CB[7] and PPY could effectively solve the problems of low conductivity of MOFs and poor stability of CPs. To verify this mechanism, we had utilized ^{1}H NMR, ROESY, ITC, and

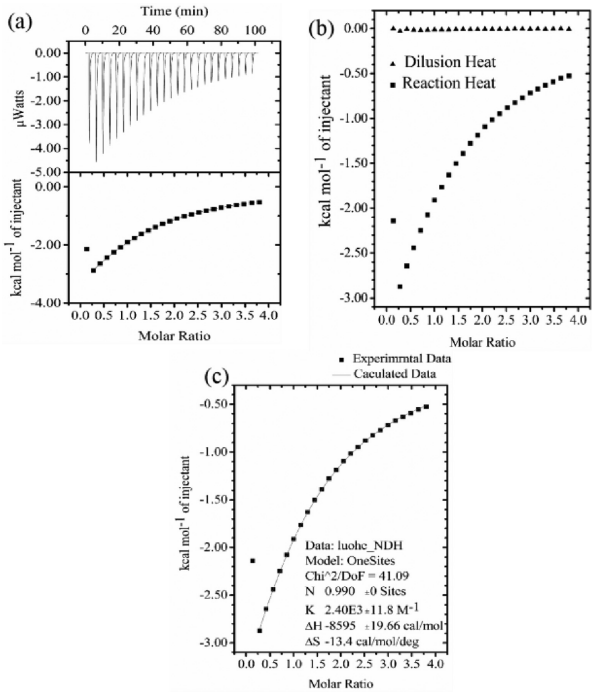

Fig. 4. Calorimetric titrations in H_2O solution (pH 7) for sequential 25 injections (10 μL per injection) of pyrrole solution (0.5 mmol/L) injecting into CB[7] solution (2.5 mmol/L): (A) raw data and apparent reaction heat; (B) heat effects of the dilution and of the complexation reaction; (C) "Net" heat effects fitted using the "one set of binding sites" model. The thermodynamic data in CB[7] ⊃ pyrrole complexation were obtained as $K_S = (2.4 \pm 0.02) \times 10^3$ mol/L.

SEM to investigate the construction of the assemblies and the morphology of electrode. The binding stoichiometry between CB[7] and pyrrole was determined to be 1:1 according to the Job's plot (Fig. S3 in Supporting information). The association constant (K_a), extracted from the ITC, was fitted as $(2.4 \pm 0.02) \times 10^3$ mol/L, the entropy and enthalpy changes were both positve, illustrating that the CB[7]⊃pyrrole complexation was mainly influenced by entropy increase (Fig. 4). The complexation and CB[7]-PPY assemblies were also determined by ^{1}H NMR and ROESY (Figs. S4–S6 in Supporting information). Fig. S5 showed that the signals of pyrrole were clearly shifted upfield ($\Delta\delta$ = 0.74 ppm), after polymerization and encapsulation by CB[7]. The 2D ROESY NMR spectra (Fig. S6) showed the rotating ROE intercorrelations between the inner protons of the CB[7] and protons of the PPY group, thus demonstrating that PPY penetrated into the CB[7] cavities.

SEM images (Fig. 1) revealed that an extraordinary morphology change took place on the surface of ZIF-8 crystals after electropolymerization of pyrrole and CB[7]. Compared with that of PPY-ZIF-8-CNTF, the size of CB[7]-PPY-ZIF-8-CNTF almost enlarged thirty-times (Figs. 1c and d) due to the formation of the assemblies, which not only covered the surface of the ZIF-8 crystals, but also performed as a bridge to interconnect the discrete ZIF-8 particles, leading to an exceptional electrochemical performance of CB[7]-PPY-ZIF-8-CNTF. The powder X-ray diffraction (PXRD) patterns of ZIF-8-CNTF and CB[7]-PPY-ZIF-8-CNTF were almostly unanimous with that of the original ZIF-8, illustrating that the electrodes still maintained the crystal and topological structure of ZIF-8 after coating and electropolymerization (Fig. S7 in Supporting information).

To further illustrate the cycling stability, the cycle life test was put into practice by CV measurement at 50 mV/s for 2000 cycles (Fig. 5a). It was evidently that the electrode can still reach 83.1% of

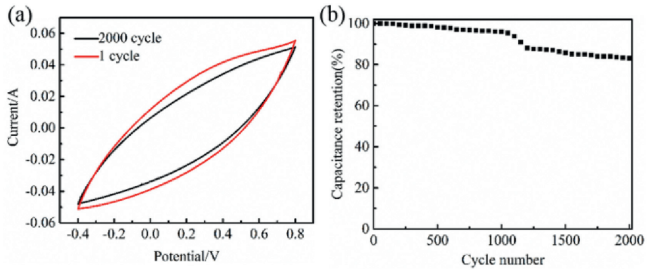

Fig. 5. (a) CV curves before and after 2000 cycles; (b) Areal capacitance retention rate of electrode after 2000 cycles.

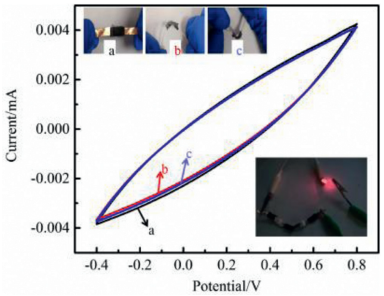

Fig. 6. CV curves of the CB[7]-PPY-ZIF-8-CNTF solid-state SC device at 50 mV/s under different conditions.

the initial areal capacitance and a good retention rate even after 2000 cycles, indicated that CB[7]-PPY-ZIF-8-CNTF device had a satisfactory cycling stability (Fig. 5b).

We also assembled and tested the supercapacitor consisted of a sulfuric acid electrolyte gel and two identical CB[7]-PPY-ZIF-8-CNTF electrode at different bending conditions in Fig. 6. It should be noted that the electrochemical performance of the capacitor was not affected by the bending angle, which indicated its high flexibility and satisfactory stability.

In summary, we illustrated an effective strategy to devise and manufacture several flexible supercapacitors, constructed from macrocycles and PPY by interconnecting ZIF-8 crystals that were anchored on carbon nanotube film with electrochemically polymerized supramolecular assemblies. Among the five macrocyclic molecules tested, CB[7] could realize an extraordinary high areal capacitance of 1533 mF/cm^2 at 5 mV/s. Due to the good solubilization and the good bonding ability to pyrrole cation radical, CB[7] could improve the electrochemical deposition efficiency of pyrrole and enhance the stability of polypyrrole cation free radical. This may pave a new way for improving the stability of conductive polymers and opening up the application of supramolecular chemistry in supercapacitors.

Declaration of competing interest

The authors report no declarations of interest.

Acknowledgment

We thank National Natural Science Foundation of China (Nos. 21971127, 21772099 and 21861132001) for financial support.

Appendix A. Supplementary data

Supplementary material related to this article can be found, in the online version, at doi:https://doi.org/10.1016/j.cclet.2021.03.002.

References

[1] L. Chen, Y. Chen, H.G. Fu, et al., Adv. Sci. 7 (2020) 2000803.
[2] R.J. Dong, Y.F. Zhou, X.H. Huang, et al., Adv. Mater. 27 (2015) 498–526.
[3] T.X. Xiao, L. Zhou, X.Q. Sun, et al., Chin. Chem. Lett. 31 (2020) 1–9.
[4] J. Shi, Y. Chen, C.F. Ke, et al., Angew. Chem. Int. Ed. 47 (2008) 7293–7296.
[5] N. Song, Z.J. Zhang, P.Y. Liu, et al., Adv. Mater. 32 (2020) 2004208.
[6] P.Y. Li, Y. Chen, Y. Liu, Chin. Chem. Lett. 30 (2019) 1190–1197.
[7] D.H. Qu, Q.C. Wang, Q.W. Zhang, et al., Chem. Rev. 115 (2015) 7543–7588.
[8] L. Feng, S.S. Jia, Y. Chen, et al., Chem. Eur. J. 26 (2020) 14080–14084.
[9] L. Shao, J.F. Sun, B. Hua, et al., Chem. Commun. 54 (2018) 4866–4869.
[10] O. Ikkala, G.T. Brinke, Science 295 (2003) 2407–2409.
[11] Q. Zhang, D.H. Qu, Q.C. Wang, et al., Angew. Chem. Int. Ed. 54 (2015) 15789–15793.
[12] P. Cordier, F. Tournilhac, C. Soulié-Ziakovic, Nature 451 (2013) 977–980.
[13] J. Ye, R.M. Zhang, W.J. Yang, et al., Chin. Chem. Lett. 31 (2020) 1550–1553.
[14] P.L. Anelli, M. Asakawa, P.R. Ashton, et al., Chem. Eur. J. 3 (1997) 1113–1135.
[15] Y.Y. Jin, Y.Q. Wang, J. Yang, et al., Cell Rep. Phys. Sci. 1 (2020) 100173.
[16] G.P. Sun, Z.M. He, M. Hao, et al., Chem. Commun. 55 (2019) 10892–10895.
[17] L.L. Tan, M.Y. Wei, L. Shang, et al., Adv. Funct. Mater. (2020) 2007277.
[18] P.R. Joan, S.G. Rafael, I. Stead, et al., Macromolecules 52 (2019) 1458–1468.
[19] S.D.P. Fielden, D.A. Leigh, C.T. McTernan, et al., J. Am. Chem. Soc. 140 (2018) 6049–6052.
[20] C.C. Zhang, X.L. Liu, Y.P. Liu, et al., Chem. Mater. 32 (2020) 8724–8732.
[21] S. Angelos, Y.W. Yang, K. Patel, et al., Angew. Chem. 120 (2008) 2254–2258.
[22] Y.L. Sun, B.J. Yang, X.A. Sean, et al., Chem. Eur. J. 18 (2012) 9212–9216.
[23] O. Reany, A. Li, M. Yefet, et al., J. Am. Chem. Soc. 139 (2017) 8138–8145.
[24] W.H. Wang, Q. Gao, A.L. Li, et al., Chin. Chem. Lett. 29 (2018) 336–338.
[25] W.J. Gong, J. Ma, Z.Y. Zhao, et al., J. Org. Chem. 82 (2017) 3298–3301.
[26] S.K. Kim, K.M. Park, K. Singha, et al., Chem. Commun. 46 (2010) 692–694.
[27] S.W. Choi, J.W. Lee, Y.H. Ko, et al., Macromolecules 35 (2002) 3526–3531.
[28] D. Tuncel, J.H.G. Steinke, Chem. Commun. (1999) 1509–1510.
[29] D. Tuncel, J.H.G. Steinke, Chem. Commun. (2001) 253–254.
[30] Y.H. Ling, A.E. Kaifer, Chem. Mater. 18 (2006) 5944–5949.
[31] Y.C. Zhang, L. Chen, H. Wang, et al., Chin. Chem. Lett. 27 (2016) 817–821.
[32] C. Yang, J. Xu, D.D. Yang, et al., Chin. Chem. Lett. 29 (2018) 1421–1424.
[33] Z.S. Lv, Y.X. Tang, Z.Q. Zhu, et al., Adv. Mater. 30 (2018) 1805468.